ISBN: 978-3-95450-214-1 ISSN: 2673-5490 doi:10.18429/JACoW-IPAC2021-MOPAB096

ROCKING CURVE IMAGING EXPERIMENT AT SSRL 10-2 BEAMLINE

A. Halavanau, J. MacArthur, R. Margraf, Z. Qu, G. Marcus, T. Sato and D. Zhu
SLAC National Accelerator Laboratory, Stanford University, Menlo Park CA , USA
C. Takacs, R. Arthur, B. Johnson, T. Rabedeau, Stanford Synchrotron Radiation Lightsource,
SLAC National Accelerator Laboratory, Stanford University, Menlo Park CA, USA

Abstract

Stanford Synchrotron Radiation Lightsource (SSRL) serves a wide scientific community with its variety of X-ray capabilities. Recently, we have employed a wiggler source located at beamline 10-2 to perform high resolution rocking curve imaging (RCI) of diamond and silicon crystals. In-house X-ray RCI capability is important for the upcoming cavity-based X-ray source development projects at SLAC, such as cavity-based XFEL (CBXFEL) and X-ray laser oscillator (XLO). In this proceeding, we describe theoretical considerations, and provide experimental results, validating the design of our apparatus. We also provide a plan for future improvements of the RCI@SSRL program.

INTRODUCTION

X-ray cavities, based on Bragg crystals, are the CBXFEL, X-ray free-electron laser oscillator (XFELO), XLO and other cavity-based X-ray sources [1–3]. In these projects, Bragg crystals define the spectral bandwidth, radiation wavefront properties, and are generally required to be of highest optical quality. Diamond and silicon crystals are often chosen due to their high lattice uniformity and excellent reflectivity in hard X-ray range. In this proceeding, we describe an experimental setup for crystal measurement and qualification, based on a commonly known technique of rocking curve imaging (RCI).

According to the theory of dynamic diffraction, a flat perfect crystal transforms an incident electric field E_i in Bragg geometry as [4–7]:

$$E_{\vec{H}} = RE_i, \tag{1}$$

where $\vec{H}$ is the reciprocal lattice vector and R is a complex reflectivity coefficient given by:

$$R(\Delta\theta, \theta, \omega) = \eta - sgn\left[\mathrm{Re}(\eta)\right]\sqrt{\eta^2 - 1}\sqrt{\frac{|F_H|}{|F_{\bar{H}}|}}, \tag{2}$$

and η is given by:

$$\eta(\Delta\theta, \theta, \omega) = \frac{(-\Delta\theta + \tan\theta\ \Delta\omega/\omega_0)\sin 2\theta - \Gamma F_0}{\Gamma|P|\sqrt{F_H F_{\bar{H}}}}. \tag{3}$$

Here F_0, F_H are the components of the structure factor, θ is the Bragg angle, P=1 for σ polarization and $\cos 2\theta$ for π polarization, $\Gamma = \frac{r_e\lambda^2}{\pi d^3}$, where r_e is the classical radius of electron and d is interplanar distance or d-spacing. Structure factors can be calculated from the atomic scattering factors and are well tabulated for a wide range of photon energies, see e.g. Refs [8–10]. A profile of $|R(\Delta\theta, \omega_0)|^2$ for a fixed photon energy ω_0 is also known as a rocking curve and can be experimentally measured; see Refs [11–13]. For our first round of measurements, we designed and built a setup similar to the one at APS 1-BM beamline [11]. In our setup, X-rays from the wiggler source are propagated through a double crystal monochromator followed by an asymmetrically cut analyzer crystal in dispersive geometry; see Fig. 1. The purpose of the asymmetrically cut crystal is two-fold: it collimates the source radiation whilst magnifying the radiation size in the diffraction plane. The asymmetry angle is defined by the required magnification ratio and can be evaluated from a simple equation [14]:

$$M = \frac{\sin(\theta + \theta_a)}{\sin(\theta - \theta_a)}, \tag{4}$$

where θ_a is the angle of asymmetry. For instance, in the experiment we used Si 531 analyzer crystal at 1.888 degrees grazing incidence, therefore $\theta_a = 41.38$ and $M = 21$.

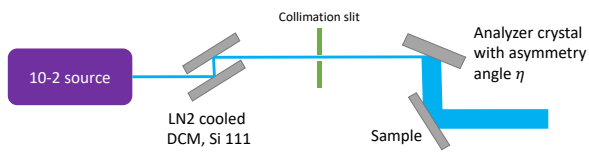

Figure 1: Experimental schematics of the SSRL RCI setup: 10-2 wiggler radiation is monochromatized at 9.83 keV via double crystal monochromator (DCM), expanded and collimated with an asymmetric Si 531 analyzer crystal. The diamond sample is rocked around its (004) reflection, at about 45 degrees.

The analyzer crystal is the highest diffraction grade Silicon, due to its nearly perfectly periodic defect-free lattice. Typically, the process of RCI is described with the help of DuMond diagrams [15]. In order to measure the narrowest rocking curve, the analyzer's reflection plane (and the corresponding set of Miller indices (hkl)) must be selected such that its d-spacing matches sample's as close as possible. For example, lattice constant of diamond is a_C=3.567 Å, Silicon is a_{Si}=5.431 Å, and the d-spacing can be calculated from $d = \sqrt{a^2/(h^2 + k^2 + l^2)}$. A proper choice of analyzer's Miller indices minimizes the expression $(h_{Si}^2 + k_{Si}^2 + l_{Si}^2) - (a_{Si}/a_C)^2(h_C^2 + k_C^2 + l_C^2)$. In this case, diamond C*(400) sample requires Si (531) analyzer. For

ISBN: 978-3-95450-214-1 ISSN: 2673-5490 doi:10.18429/JACoW-IPAC2021-MOPAB096

more combinations of diamond reflections and corresponding analyzers, we refer the reader to Table 1. It is instructive to calculate theoretical width of the rocking curve (dubbed Darwin width) via:

$$\Delta\Theta = \left|\Gamma\sqrt{F_H F_{\bar{H}}}\tan\theta/(2.0\sin^2\theta)\right|. \quad (5)$$

The angular step size of the sample motion stage $\Delta\theta_r \ll \Delta\Theta$, in order for the rocking curve to be well resolved. We typically rotated the samples by 0.87 µrad per measurement.

Table 1: Different Diamond Reflections, Corresponding Silicon Analyzers and Characterization Photon Energies, Accessible at the SSRL 10-2 Beamline

C*	Si	θ_a	ω (keV)	$\Delta\Theta$ (μrad)	L_{e_σ} (m)
400	531	41.38	9.83	8.2	9.85
800	777	42.74	19.66	1.3	31.74
220	331	43.70	6.95	20.7	5.49
440	555	43.30	13.90	3.4	16.74
333	800	43.64	12.77	3.0	20.69

A salient feature of our setup is the high average brightness of SSRL 10-2 wiggler source. Due to its 15 period wiggler, one obtains a 30-fold increase in flux, compared to a single SSRL bending magnet; see Fig. 2. High photon flux at 9.831 keV allowed for 1-2 s exposure times per angular point, hence the entire rocking curve was imaged in a few minutes with 1X optical magnification. Our setup permits for rapid crystal screening, which is especially valuable for iterative crystal mounting, drumhead crystals [16] and cooling studies.

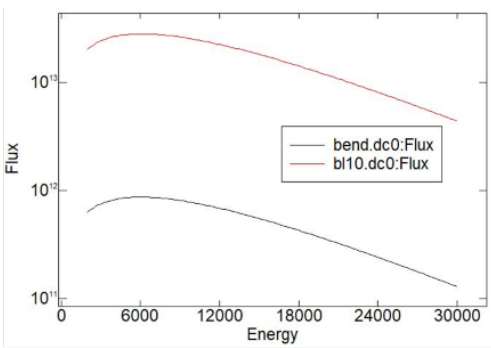

Figure 2: Spectral flux of SSRL bending manget and 10-2 wiggler as a function of photon energy.

EXPERIMENTAL APPARATUS

SSRL 10-2 wiggler beamline was operated in the unfocused configuration with a Si (111) liquid nitrogen cooled double crystal monochromator (DCM). The DCM was tuned to a photon energy of 9.831 keV, matching the CBXFEL project requirement. A CAD schematic of the motion stack used during the beamtime is shown in Fig. 3, while a picture

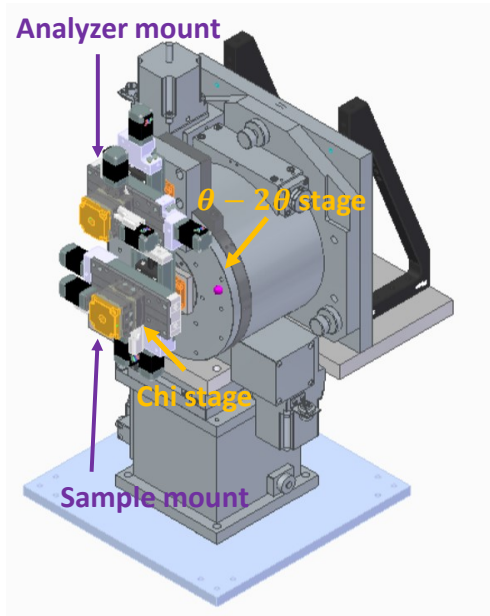

Figure 3: CAD rendering of motion stages used for rocking curve imaging.

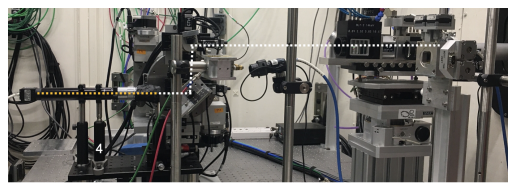

Figure 4: X-ray path (right to left) in the hutch (white) and visible light from the YAG (yellow).

of the X-ray path in the hutch is shown in Fig. 4. We used Kohzu RA-2021 theta-2-theta stage mounted on top of the vertical and horizontal Kohzu translation stages to position the collimator crystal into the incoming beam. An xy/tip-tilt stack of Zaber stages was used to set the collimator position and out-of-plane angle (chi). Following the collimator, the X-ray beam footprint overfilled the diamond sample.

A 200 micron thick YAG screen was used to convert the diffracted X-rays into an optical signal. A 1× magnification objective was used to transport the optical signal to a FLIR camera. The camera has a pixel size of 3.45 microns.

DATA ANALYSIS

Here we show typical measurements of Si (531) and C*(400) crystal samples. To validate our setup, we started with the flat stress-free Si crystal, which is expected to be strain free and show a uniform distribution of the rocking curve center distribution in the RCI map. We scanned the Si crystal over 30.5 µrad using Chi stage, adjusting it in theta each time to meet the Bragg condition, until we found the condition for the flattest rocking curve center map. We then scanned the crystal over 23.56 µrad in steps of 0.87 µrad, with a 1.7 s exposure time per step. The resulting rocking curves and their center is plotted in Figs. 5 and 6 a) and is

ISBN: 978-3-95450-214-1 ISSN: 2673-5490 doi:10.18429/JACoW-IPAC2021-MOPAB096

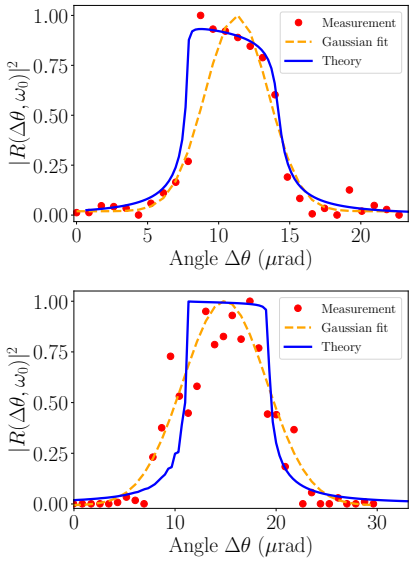

Figure 5: Example single pixel rocking curves for Si 531 (a) and C 400 (b) crystal samples.

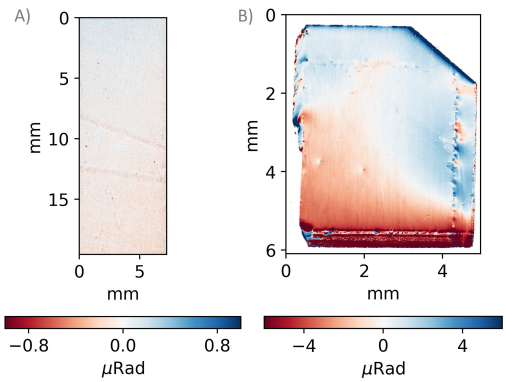

Figure 6: Rocking curve center plots for Si 531 (a) and C 400 (b) crystal samples.

indeed confirming the expectations. We then scanned the diamond sample over 48 µrad in steps of 0.87 µrad, with a 1.7 s exposure time per step. The rocking curve center reveals dislocations and residual lattice strain, as shown in Fig. 6 b), corroborating the previous measurements of the same sample at APS-1 BM and SPring-8 1-km beamlines. To analyze our rocking curve scans, we fit a Gaussian function to the rocking curve for each image pixel as a function of angle, as shown in Fig. 5. An example of the rocking curve center plot is shown in Fig. 6.

In case of Silicon crystal it shows very good lattice uniformity and practically no lattice strain. For the diamond sample, we identified that it was bent in the vertical direction, with a relatively flat area in the center. This type of measurements allow quick assessment of the optical quality of the diamond pertaining its future application.

FUTURE IMPROVEMENTS

Due to sufficient photon flux across a wide range of photon energies (see Fig. 2), it is possible to perform RCI measurements for other diamond reflections. We have summarized these possibilities in Table 1. These measurements will allow to probe different depths of the crystal due to the difference in extinction lengths.

During the measurements, the diamond samples were constrained with a kapton tape. Some crystals, especially thin ones, were found drifting in the crystal holder. We are now designing a new stress-free holder to improve sample stability and minimize the mechanical drifting.

SUMMARY

We have successfully commissioned X-ray rocking curve imaging setup for Diamond and Silicon crystals. Our setup utilizes SSRL beamline 10-2 wiggler, double crystal Silicon monochromator and an asymmetric Silicon crystal analyzer. We specifically optimized the time of single RCI measurement, to allow for rapid studies of crystal holders and cooling techniques. In the future, we envision expanding our setup to different geometries, and possibly implementing white beam topography capability.

ACKNOWLEDGEMENTS

We would like to thank Y. Shvyd'ko (ANL), Z. Huang, Y. Feng, J. Krzywinski (SLAC), A. Benediktovitch (CFEL, DESY) and U. Bergmann (University of Wisconsin) for many valuable tips and suggestions during the design and the first experiment. This work is supported by the U.S.Department of Energy Contract No. DE-AC02-76SF00515.

REFERENCES

[1] K.-J. Kim, Y. Shvyd'ko, and S. Reiche, "A proposal for an X-ray free-electron laser oscillator with an energy-recovery Linac", *Phys. Rev. Lett.*, vol. 100, p. 244 802, Jun. 2008. doi:10.1103/PhysRevLett.100.244802

[2] G. Marcus *et al.*, "Refractive guide switching a regenerative amplifier free-electron laser for high peak and average power hard X-rays", *Phys. Rev. Lett.*, vol. 125, p. 254 801, Dec. 2020. doi:10.1103/PhysRevLett.125.254801

[3] A. Halavanau *et al.*, "Population inversion X-ray laser oscillator", *Proc. Nat. Acad. Sci.*, vol. 117, no. 27, pp. 15 511–15 516, 2020. doi:10.1073/pnas.2005360117

[4] W. H. Zachariasen and E. L. Hill, "The theory of X-ray diffraction in crystals", *Am. J. Phys. Chem.*, vol. 50, no. 3, pp. 289–290, Mar. 1946. doi:10.1021/j150447a024

[5] B. W. Batterman and H. Cole, "Dynamical diffraction of X-rays by perfect crystals", *Rev. Mod. Phys.*, vol. 36, pp. 681–717, Jul. 1964. doi:10.1103/RevModPhys.36.681

ISBN: 978-3-95450-214-1 ISSN: 2673-5490 doi:10.18429/JACoW-IPAC2021-MOPAB096

[6] Y. Shvyd'ko and R. Lindberg, "Spatiotemporal response of crystals in X-ray Bragg diffraction", *Phys. Rev. ST Accel. Beams*, vol. 15, p. 100 702, Oct. 2012. doi:10.1103/PhysRevSTAB.15.100702

[7] R. R. Lindberg and Y. V. Shvyd'ko, "Time dependence of Bragg forward scattering and self-seeding of hard X-ray free-electron lasers", *Phys. Rev. ST Accel. Beams*, vol. 15, p. 050 706, May 2012. doi:10.1103/PhysRevSTAB.15.050706

[8] J. P. Sutter, O. Chubar, and A. Suvorov, "Perfect crystal propagator for physical optics simulations with Synchrotron Radiation Workshop", in *Proc. Advances in Computational Methods for X-Ray Optics III*, San Diego, CA, United States, Sep. 2014, pp. 171–185. doi:10.1117/12.2061646

[9] D. T. Cromer and J. B. Mann, "X-ray scattering factors computed from numerical hartree–fock wave functions", *Acta Crystallogr. A*, vol. 24, no. 2, pp. 321–324, 1968. doi:10.1107/S0567739468000550

[10] C. T. Chantler, "Theoretical form factor, attenuation, and scattering tabulation for Z=1–92 from E=1–10 eV to E=0.4–1.0 MeV", *J. Phys. Chem. Ref. Data*, vol. 24, no. 1, pp. 71–643, 1995. doi:10.1063/1.555974

[11] A. Macrander *et al.*, "X-ray optics testing beamline 1-BM at the advanced photon source", *AIP Conf. Proc.*, vol. 1741, no. 1, p. 030 030, 2016. doi:10.1063/1.4952853

[12] P. Pradhan *et al.*, "Small Bragg-plane slope errors revealed in synthetic diamond crystals", *J. Synchrotron Radiat.*, vol. 27, no. 6, pp. 1553–1563, Nov. 2020. doi:10.1107/S1600577520012746

[13] K. Tamasaku, T. Ueda, D. Miwa, and T. Ishikawa, "Goniometric and topographic characterization of synthetic IIa diamonds", *J. Phys. D Appl. Phys.*, vol. 38, pp. A61–A66, May 2005. doi:10.1088/0022-3727/38/10a/012

[14] S. Stoupin *et al.*, "Sequential X-ray diffraction topography at 1-bm x-ray optics testing beamline at the advanced photon source", *AIP Conf. Proc.*, vol. 1741, no. 1, p. 050 020, 2016. doi:10.1063/1.4952940

[15] Y. Shyd'ko, *X-Ray Optics: High-Energy-Resolution Applications*. Berlin Heidelberg, Germany: Springer, 2004.

[16] T. Kolodziej, P. Vodnala, S. Terentyev, V. Blank, and Y. Shvyd'ko, "Diamond drumhead crystals for X-ray optics applications", *J. Appl. Crystallogr.*, vol. 49, no. 4, pp. 1240–1244, Aug. 2016. doi:10.1107/S1600576716009171